



Histological and Immunohistochemical Study on the Effects of *Astragalus Membranaceus* versus Adipose Tissue-Derived Stem Cells in Thioacetamide Induced Liver Fibrosis in Male Albino Rats

Seham Abdel Hamid El Kalawy¹, Mohamed Salah Elgendy², Laila Ahmed Rashed³, Abeer Ibraheem Abd Allah Omar¹, Maryham George Loka Yacoub²

¹Histology Department, Faculty of Medicine, Cairo University, Cairo, Egypt

²Histology Department, Faculty of Medicine, Fayoum University, Fayoum, Egypt

³Biochemistry Department, Faculty of Medicine, Cairo University, Cairo, Egypt

drmamyham_5682@yahoo.com

Abstract: Background: Liver fibrosis is one of the common complications of acute hepatitis. Thioacetamide (TAA) is a strong hepatotoxic agent inducing experimental liver fibrosis. Adipose derived mesenchymal stem cells (AD-MSCs) had potent antifibrotic and regenerative effects. *Astragalus membranaceus* (AM), one of the Herbal Chinese medicine, was reported to protect the liver and regulate its functions. **Aim of work:** Comparing the effect of AM versus autologous rat AD-MSCs on TAA-induced fibrotic rat liver and hepatic stellate cells (HSCs) activation, in adult male albino rats. **Materials and Methods:** Forty five male albino rats were divided into three groups: group I (control group), group II (untreated TAA group); received IP injection of 200 mg/Kg of TAA three times weekly for 8 weeks, group III (treated group); treated as group II. Then at the beginning of 5th week till the end of 8th week, each rat received either single daily oral dose (500 mg/kg) of AM (subgroup IIIa) or single IP injection of PKH26 labeled rat AD-MSCs (3×10^6 cells) (subgroup IIIb). Biochemical and statistical analysis of AST, ALT, Albumin and procollagen were done. Liver sections were subjected to H & E, Mallory trichrome stains and immunohistochemical stains for α -SMA & NF- κ B. Morphometric measurement of mean area % of collagen, α -SMA and NF- κ B were done followed by statistical analysis. **Results:** Histological, morphometric and statistical results revealed disorganization of the lobular architecture, features of hepatocyte injury and fibrotic changes in group II. The treated group showed improvement of the hepatic lesion, reduction of fibrosis and proper lobular organization. This improvement was more obvious in stem cells treated subgroup. **Conclusion:** Administration of AD-MSCs has more improving effect on TAA-induced liver fibrosis in rat than *Astragalus* where MSCs are more potent anti-inflammatory and anti-fibrotic.

[Seham Abdel Hamid El Kalawy, Mohamed Salah Elgendy, Laila Ahmed Rashed, Abeer Ibraheem Abd Allah Omar, Maryham George Loka Yacoub. **Histological and Immunohistochemical Study on the Effects of *Astragalus Membranaceus* versus Adipose Tissue-Derived Stem Cells in Thioacetamide Induced Liver Fibrosis in Male Albino Rats.** *J Am Sci* 2019;15(10):15-26]. ISSN 1545-1003 (print); ISSN 2375-7264 (online). <http://www.jofamericanscience.org>. 3. doi:[10.7537/marsjas151019.03](https://doi.org/10.7537/marsjas151019.03).

Key Words: Liver fibrosis, Thioacetamide, *Astragalus membranaceus*, Adipose derived mesenchymal stem cells.

1. Introduction:

The liver is one of the most important organs in the human body. It controls homeostasis through controlling lipids, carbohydrates and proteins metabolism. Additionally, it produces plasma proteins as albumin, fibrinogen, prothrombin, lipoproteins and α - and β -globulins. Moreover, the hepatocytes are involved in degradation of the hydrophobic drugs and toxins where they convert these substances into more soluble ones (Ross & Pawlina, 2016).

Liver fibrosis could be induced by different causes like toxins, alcohol, viruses and drugs (Lee and Friedman, 2011). Advanced liver fibrosis results in cirrhosis where there is conversion of normal liver architecture into structurally abnormal nodules with

subsequent hepatocellular dysfunction (Gines, et al., 2004 & Liedtke et al, 2013).

Hepatic stellate cells (HSCs) are Ito cells present in the space of Disse. They remain quiescent in healthy liver (Blaner et al., 2009). With liver injury, HSCs were reported to be activated and transdifferentiated into myofibroblast-like cells with expression of alpha smooth muscle actin (α -SMA) (Ionescu et al., 2013). Such transdifferentiation is considered the key for pathogenic liver fibrosis through production of fibrotic extracellular matrix (Bataller and Brenner, 2005).

Experimentally, liver fibrosis could be induced by thioacetamide (TAA), a potent hepatotoxic agent, which is metabolized to reactive acetamide and TAA-S-oxide. Such metabolites combine covalently with

the hepatic tissue macromolecules leading to accumulation of fatty acids, damage of proteins and DNA with subsequent production of reactive oxygen species (ROS) and persistent hepatic oxidative stress (OS) that may progress to liver failure (Abdou et al, 2015, Al-Attar & Shawush., 2015).

The most effective treatment for end stage hepatic failure is liver transplantation. However, this way of treatment is restricted by the shortage of donors and the long-term use of immunosuppressive drugs (Miryounesi et al., 2013).

Mesenchymal stem cells (MSCs), a prominent source in regenerative medicine and cell therapy, provided an effective treatment in cases of liver impairment (Puglisi et al., 2011). They could be isolated from different tissues as adipose tissue (Zuk et al, 2002). Adipose tissue-derived mesenchymal stem cells (ADMSCs) are much more effective than other sources of MSCs being more abundant and easily obtained. Moreover, they could be maintained longer in culture with higher proliferative capacity (Bunnell et al, 2008).

Astragalus membranaceus (AM) is the dried root of leguminous plant *Mongolia Astragalus* as described in the Chinese book (Yang et al, 2005). It was reported that Astragalus can resist collagen deposition and treat development of organ fibrosis via inhibition of alpha smooth muscle actin (α -SMA) and transforming growth factor β -1 (TGF- β 1) expressions (Meng et al, 2011). Furthermore, the flavonoids extracted from Astragalus were proved to be useful in preventing rat liver fibrosis induced by dimethylnitrosamine (DMN) (Cheng et al., 2017).

This study aimed to compare the therapeutic effect of AM (the traditional Chinese medicinal herb) versus autologous rat ADMSCs on TAA-induced liver fibrosis and HSCs activation, in adult male albino rats.

2. Materials and methods:

I) Animals:

Forty five adult male albino rats (180 – 200 g) were treated according to Cairo University Animal Use Committee guidelines. They were housed at the animal house, Faculty of Medicine, Cairo University. The animals were bred in wire mesh cages at 24±1°C and normal light/dark cycle and provided with ordinary rat chow with free water and food access.

II) Drugs used:

- **Thioacetamide (TAA):** (Loba Chemie, India), cat. number: 6259. It was provided in the form of crystalline powder in a bottle of 25gm.

- ***Astragalus membranaceus* (AM) Extract:** Traditional Chinese Medicinal Herbs, made in USA and distributed by Amazing Nutrition Hoboken NJ07030. It was supplied as soft gel capsules, each one contains 500 mg of dried extract of AM (root).

- **Immunohistochemical primary antibodies:**
 - **Alpha smooth muscle actin (α -SMA):** mouse monoclonal antibody, Lab Vision Neomarkers, U.S.A, cat. number: MS-113-R7.

- **Nuclear factor kappa-beta (NF- κ B):** rabbit polyclonal antibody, Lab Vision Neomarkers, U.S.A, cat. number: RB-9034-R7.

III) Stem cells:

Autologous rat adipose tissue derived mesenchymal stem cells (ADMSCs) were prepared at Stem Cell Research Unit at Biochemistry Department, Faculty of Medicine, Cairo University according to a previous protocol (Bunnell et al., 2008). Then ADMSCs were labelled with PKH26 red fluorescent cell linker (Sigma- Aldrich, USA) according to Sigma protocol.

IV) Experimental design:

The rats were divided into three groups:

Group I (control group, 15 rats):

The animals were subdivided into five subgroups (3 rats each):

Subgroup Ia: Each rat received IP injection of 1ml sterile distilled water three times weekly for 8 weeks.

Subgroup Ib: Rats were prepared as in subgroup Ia then they were given daily oral saline (1ml) via gastric gavage, starting from day 29 (start of the 5th week) till the end of the 8th week.

Subgroup Ic: Rats were prepared as in subgroup Ia and on day 29 (start of the 5th week), each rat received single IP injection of 1ml PBS.

Subgroup Id (Astragalus-control subgroup): Each rat received a single daily oral dose (500 mg/kg) of AM dissolved in 1ml saline via gastric gavage at the beginning of 5th week (29th day) till the end of 8th week.

Subgroup Ie (stem cell-control subgroup): Each rat received a single IP injection of PKH26-labeled ADMSCs (3x10⁶ cells/ rat suspended in 1 ml PBS) at the beginning of 5th week (29th day).

Group II (TAA group, 10 rats):

The rats received IP injection of 200 mg/kg TAA freshly dissolved in 1 ml sterile distilled water three times weekly for 8 weeks (Alshawsh et al., 2011).

Group III (treated group, 20 rats):

The animals were prepared as in subgroup II, then they were subdivided into 2 subgroups, 10 rats each:

Subgroup IIIa (Astragalus-treated subgroup): Each rat was given daily oral AM (500 mg/kg, dissolved in 1 ml saline) using a gastric tube (Tseng et al, 2016) starting from day 29 [start of the 5th week, i.e. after the start of fibrosis

Subgroup IIIb (stem cell-treated subgroup): The rats received single IP injection of PKH26-labeled ADMSCs [3x10⁶ cells/ rat, suspended in 1 ml PBS

(Miryounesi et al. 2013)] on day 29 [start of the 5th week, i.e. after the start of fibrosis.

V) Experimental procedure:

1- Biochemical investigations:

At the end of the 8th week, serum levels of Aspartate transaminase (AST), Alanine transaminase (ALT), albumin and procollagen were measured at Biochemistry Department, Faculty of Medicine, Cairo University according to previous methodologies (Soresi et al., 2014).

2- Histological studies:

All rats of all groups were sacrificed at the end of the 8th week after being anaesthetized with intraperitoneal phenobarbitone (60mg/kg). Then the liver of each rat was dissected and immediately fixed in 10% formol saline, kept for 24 h then processed to Paraffin blocks.

Six micrometers-thick sections were cut from the Paraffin blocks.

A) For light microscopical examination, sections were stained with:

Hematoxylin and Eosin (H & E) (Kiernan, 2015).

Mallory trichrome stain for detection of collagen fibers (Bancroft & Gamble, 2008).

Immunohistochemical staining (Ramos-Vara & Miller, 2014) for:

- **α -SMA:** activated hepatic stellate cells and smooth muscle cells marker (Cherng et al., 2008).
- **NF- κ B:** inflammatory transcription factor in the inflammatory cells and the inflamed hepatocytes (Algendaby, 2018).

The sections for immunohistochemical stains were boiled for 10 min in 10 mM citrate buffer (AP9003) at pH 6 for antigen retrieval then incubated for 1h with the primary antibodies. Ultravision detection system (TP-015-HD) was used to complete immunostaining and Mayer's hematoxylin (TA-060-MH) was used for counterstaining. Citrate buffer, Ultravision detection system and Mayer's hematoxylin were purchased from Lab Vision Neomarkers, USA.

B) For fluorescent microscopical examination:

Unstained sections of control subgroup Ie and subgroup IIIb were examined.

3- Morphometric studies and statistical analysis:

Ten non-overlapping fields from each subgroup were used to measure:

Mean area percent of collagen fibers: in Mallory trichrome stained sections (magnification x40).

Mean area percent of α -SMA: in anti α -SMA immunohistochemically stained sections (magnification x400).

Mean area percent of NF- κ B: in anti NF- κ B immunohistochemically stained sections (magnification x400).

These were done using Leica Qwin-500 LTD-software image analysis computer system (Cambridge, England) at Histology Department, Faculty of Medicine, Cairo University. Then morphometric and biochemical measurements were statistically analysed using "SPSS for Windows, version 16" and the data were reported as mean \pm standard deviation (SD). One-way analysis of variance (ANOVA) followed by "tuckey" post-hoc test were used to determine the statistical significance ($P < 0.05$ was considered significant) (Armitage et al., 2001).

3. Results:

General observation:

- Three rats of subgroup II died at the end of the 4th week. The dead animals were replaced by other ones so, the number of group II remained 10 rats.
- Examination of all control subgroups revealed similar histological, biochemical and morphometric results. So, they were collectively named as control group (group I).

Morphometric analysis of the biochemical results:

• The serum levels of ALT, AST & procollagen:

Group II showed significant increase versus control group. Subgroup IIIa revealed significant decrease versus group II and significant increase versus group I. However, subgroup IIIb demonstrated significant decrease when compared to subgroup IIIa and significant increase when compared to control group except for procollagen level where it showed non-significant increase when compared to control group (Table 1).

• The serum level of Albumin:

It showed significant decrease in group II and subgroup IIIa versus control group and significant increase in subgroup IIIa versus group II. However, subgroup IIIb demonstrated significant increase when compared to subgroup IIIa and significant decrease when compared to control group (Table 1).

Histological Results:

Haematoxylin and Eosin stain:

Examination of the liver sections of the control group revealed ill-defined hexagonal classic hepatic lobules with terminal hepatic venules in their centers. Hepatocytes appeared ascords radiating from the terminal hepatic venules to the periphery of the hepatic lobules where portal areas were seen. The portal area contained a branch of the bile duct lined with simple cubical epithelium; a branch of the portal vein which was the widest with thin wall and a branch of the hepatic artery with narrow lumen. The hepatocytes appeared as polygonal cells having acidophilic cytoplasm and central rounded vesicular nuclei with prominent nucleoli. Some cells were binucleated. Hepatocyte cords were separated by

blood sinusoids lined by endothelial and Kupffer cells (**Figs. 1a-1c**).

Sections of rats' livers of subgroup II (8 weeks of TAA administration) showed disorganization of the lobular architecture and thickening of the fibrous septa with inflammatory cell infiltration. The hepatic sinusoids and the terminal hepatic venule were dilated and the later had distorted wall. The branches of portal vein were congested and dilated. In zone I some hepatocytes showed deeply acidophilic cytoplasm with clumped chromatin and others were apparently normal with acidophilic cytoplasm and vesicular nuclei. Hepatocytes of zone II revealed markedly vacuolated cytoplasm; some of them demonstrated dissolved nuclei while others had shrunken and dark nuclei. Some of hepatocytes of zone III had markedly vacuolated cytoplasm, some had vesicular nuclei and others had pyknotic nuclei. The hepatic sinusoids were lined with endothelial cells and prominent Kupffer cells (**Figs. 1d-1f**).

Examination of liver sections of Astragalus-treated subgroup (subgroup IIIa) showed ill-defined lobulation with radiating cords of hepatocytes which were nearly normal. Some of the hepatocytes were binucleated. Congestion of the terminal hepatic venule & dilatation of the portal vein branches were noticed. Minimal inflammatory cell infiltration appeared around the branches of the portal vein. Endothelial and Kupffer cells were also noticed lining the slightly congested hepatic sinusoids (**Figs. 1g-1i**).

Moreover, Liver sections of stem cell-treated subgroup (subgroup IIIb) demonstrated ill-defined lobulation with radiating cords of hepatocytes which were nearly normal. Some hepatocytes were binucleated. There was slight congestion of the terminal hepatic venules & dilatation of portal vein branches. Endothelial and Kupffer cells were also noticed lining hepatic sinusoids (**Figs. 1j-1l**).

Mallory trichrome stain:

The control group showed very minimal amount of collagen fibers around the terminal hepatic venule and in the portal tracts. No interlobular septademarking the classic hepatic lobules nor collagen fibers in between the hepatocytes could be detected (**Figs. 2a & 2b**).

However, subgroup II revealed marked increase of the collagen fibers in the interlobular septa, around the terminal hepatic venule, in the portal tracts and in between the hepatocytes (**Figs. 2c & 2d**).

Sections of subgroup IIIa demonstrated minimal amounts of collagen fibers around the terminal hepatic venule, in the portal areas and in between the hepatocytes (**Figs. 2e & 2f**).

Meanwhile, sections of subgroup IIIb exhibited minimal amounts of collagen fibers around the

terminal hepatic venule, and around the branches of portal vein only (**Figs. 2g & 2h**).

Immunohistochemical results:

A) Alpha smooth muscle actin (α -SMA) immunostaining:

In the control group, positive immunoreaction was seen in the vascular wall of the portal area (branches of the portal vein & the hepatic artery) and in the wall of the terminal hepatic venules (**Figs. 3a & 3b**). In group II, this immunoreaction was extended to include HSCs present in between the hepatocytes and the hepatic lobules, surrounding the terminal hepatic venule and the branches of the portal vein. These HSCs appeared as branched, stellate cells with multiple fine processes (**Figs. 3c-3e**). However after administration of AM (subgroup IIIa) or ADMSCs (subgroup IIIb), the positive immunoreaction returned back to its normal appearance (**Figs. 3f & 3g**).

B) Nuclear factor kappa-beta (NF- κ B) immunostaining:

The examined control liver sections showing negative immunostaining in the hepatocytes around terminal hepatic venule and around the branch of portal vein (**Figs. 4a & 4b**). Sections of TAA group showed positive cytoplasmic immunoreaction in almost all hepatocytes and few inflammatory cells around terminal hepatic venule and around the branch of the portal vein, in addition to the epithelial lining of the bile duct (**Figs. 4c & 4d**). Subgroup IIIa showed positive immunoreactions in the cytoplasm of multiple hepatocytes around terminal hepatic venule and around branches of portal vein. However, inflammatory cells revealed negative immunoreaction (**Figs. 4e & 4f**). Subgroup IIIb demonstrated positive cytoplasmic immunoreaction in few hepatocytes around terminal hepatic venule. Negative immunoreaction was observed in most of the inflammatory cells around the terminal hepatic venule and in the hepatocytes and the inflammatory cells around the branch of the portal vein (**Figs. 4g & 4h**).

Examination of liver sections under fluorescence microscope:

Fluorescent signals (indicating PKH26 labeled ADMSCs) were absent in the liver parenchyma of the stem cells control subgroup (Ie) (**Fig. 5a**). They were observed in stem cell-treated subgroup IIIb in the liver parenchyma (**Fig. 5b**).

Morphometric results:

The mean area % of collagen fibers and that of positive immunoreactions for α -SMA and NF- κ B showed significant increase in group II versus control group. Astragalus-treated subgroup (IIIa) revealed significant decrease versus group II and significant increase versus group I. However, stem cell-treated subgroup (IIIb) demonstrated significant decrease when compared to subgroup IIIa and non-significant

increase when compared to control group except for NF- κ B immunoreaction where it showed significant

increase when compared to control group (Table 1).

Table 1: Morphometric analysis of the mean \pm SD of the biochemical results and the area % of collagen, α -SMA and NF- κ B

	Control group	Group II	Subgroup IIIa	Subgroup IIIb
ALT (IU/L)	15.67 \pm 1.53	85.00 \pm 3.00 ^{##}	37.00 \pm 1.00 ^{##S}	28.00 \pm 1.00 ^{##So}
AST (IU/L)	12.00 \pm 1.00	83.33 \pm 3.06 ^{##}	28.00 \pm 1.01 ^{##S}	20.23 \pm 1.51 ^{##So}
Albumin (g/dl)	5.13 \pm 0.21	2.06 \pm 0.03 ^{##}	3.53 \pm 0.40 ^{##S}	4.43 \pm 0.31 ^{##So}
Procollagen (U/ML)	32.45 \pm 1.80	119.20 \pm 0.66 ^{##}	50.97 \pm 0.61 ^{##S}	35.40 \pm 2.44 ^{##So}
Collagen area %	1.61 \pm 0.83	31.89 \pm 2.78 ^{##}	6.85 \pm 1.06 ^{##S}	2.8 \pm 0.81 ^{##So}
α -SMA area %	1.91 \pm 0.40	29.48 \pm 3.72 ^{##}	4.60 \pm 0.59 ^{##S}	2.41 \pm 1.03 ^{##So}
NF- κ B area %	Not detected	30.85 \pm 1.01 ^{##}	5.72 \pm 1.34 ^{##S}	3.57 \pm 0.64 ^{##So}

*Significant compared to control #Significant compared to subgroup IIa \$ Significant compared to subgroup IIIa

°Significant compared to subgroup IIIa

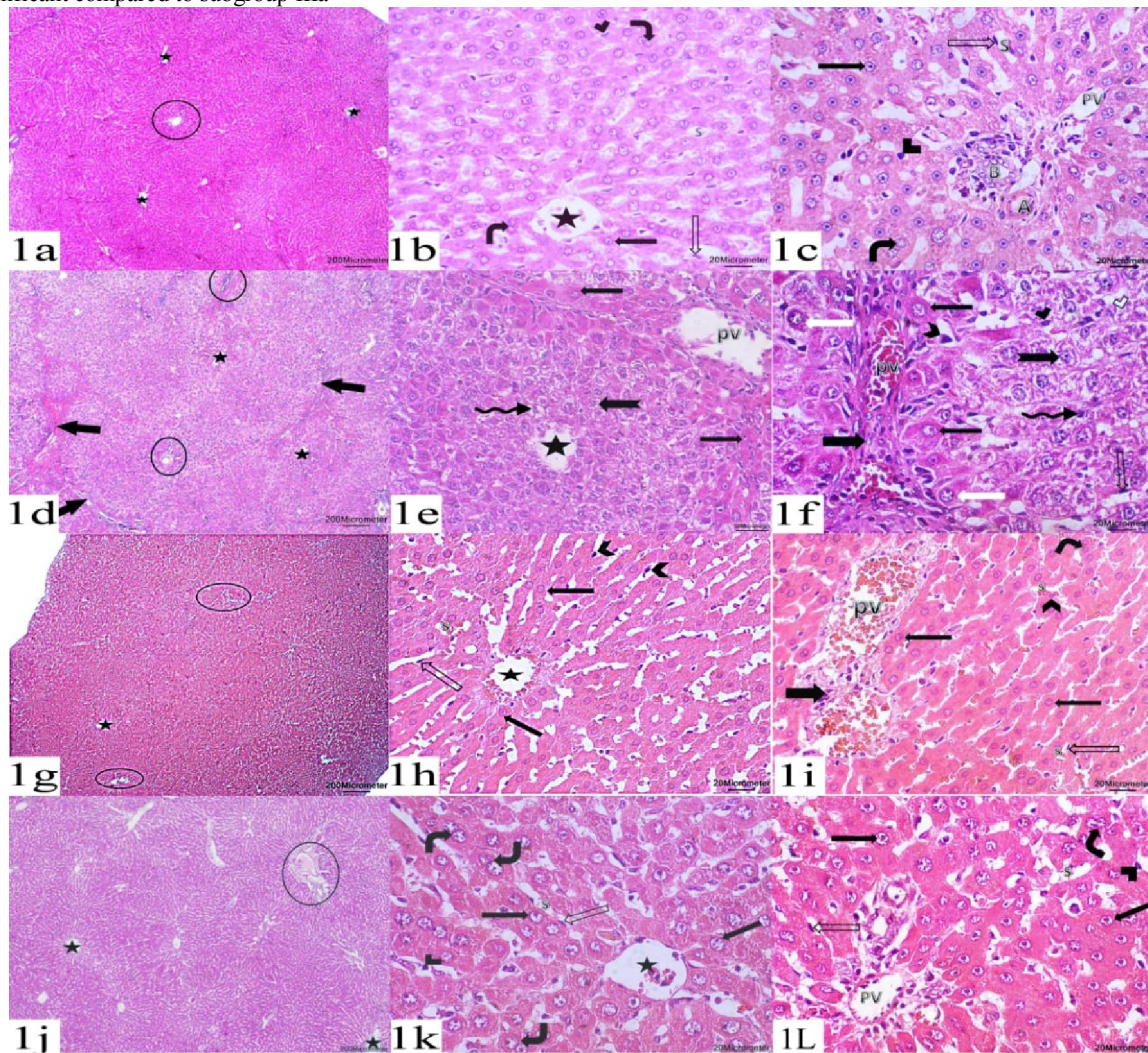


Figure 1: Photomicrographs of liver sections show terminal hepatic venule (star), portal area (encircled) that contains a branch of bile duct (B), a branch of portal vein (PV) & a branch of hepatic artery (A). The hepatocytes appear either normally (thin arrows), binucleated (curved arrows), with vacuolated cytoplasm (bifid arrows), with pyknotic nuclei (wavy arrows), with deeply acidophilic cytoplasm and clumped chromatin (white arrows) or with dissolved nuclei (white arrow head). The hepatocytes' cords are separated by blood sinusoids (S) that are lined with endothelial cells (hollow arrows) & Kupffer cells (black arrow heads). Some photomicrographs reveal thick connective tissue septa with mononuclear infiltration (thick arrows). [Group I (a-c), group II (d-f), subgroup IIIa (g-i), subgroup IIIb (j-l)]. [H & E, x40 (a, d, g & j), x200 (e), x400 (b, c, f, h, I, k & l)]

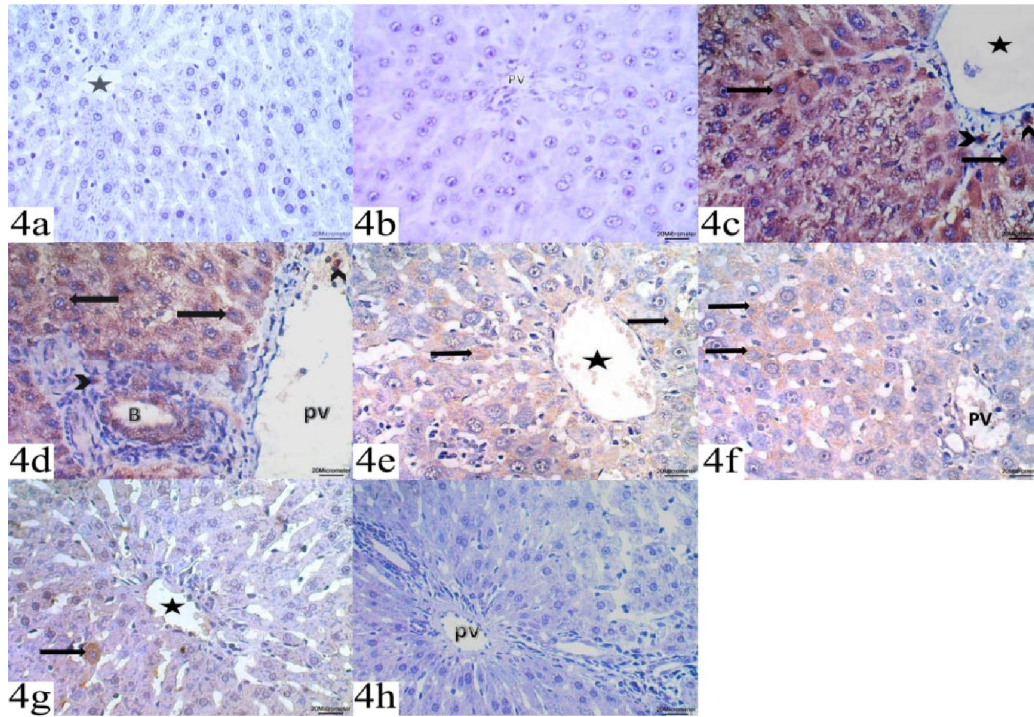


Figure 2: Photomicrographs of liver sections show collagen fibers in the portal area (encircled), around the portal vein (bifid arrows), around the terminal hepatic venule (arrow head), in the connective tissue septa (thin arrows) and in-between hepatocytes (thick arrows). [Group I (a & b), group II (c & d), subgroup IIIa (e & f), subgroup IIIb (g & h)]. [Mallory trichrome, x40 (a, c, e & g), x200 (b, d, f & h)]

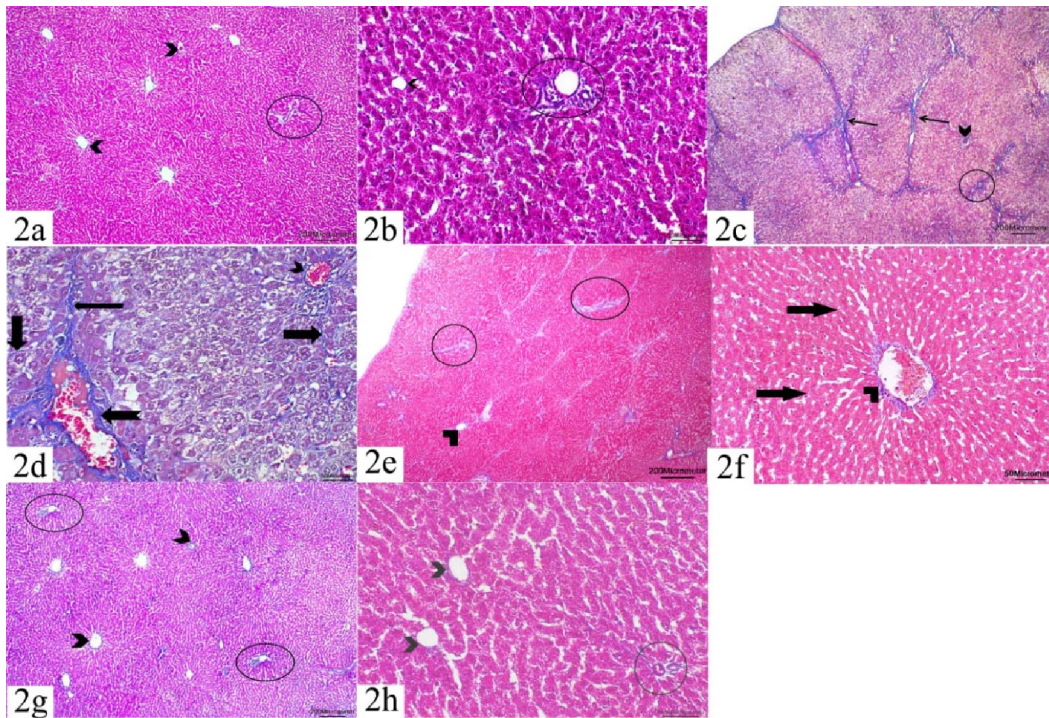


Figure 3: Photomicrographs of liver sections show positive immunoreaction (thin arrows), positive immunoreaction in the portal area (encircled), in-between hepatocytes (arrow heads) and in stellate cells (thick arrows). [Group I (a & b), group II (c-e), group III (f & g)]. [α -SMA, x100 (c), x400 (a, b & d-g)], Inset photomicrographs [α -SMA, x1000 (d & e)]

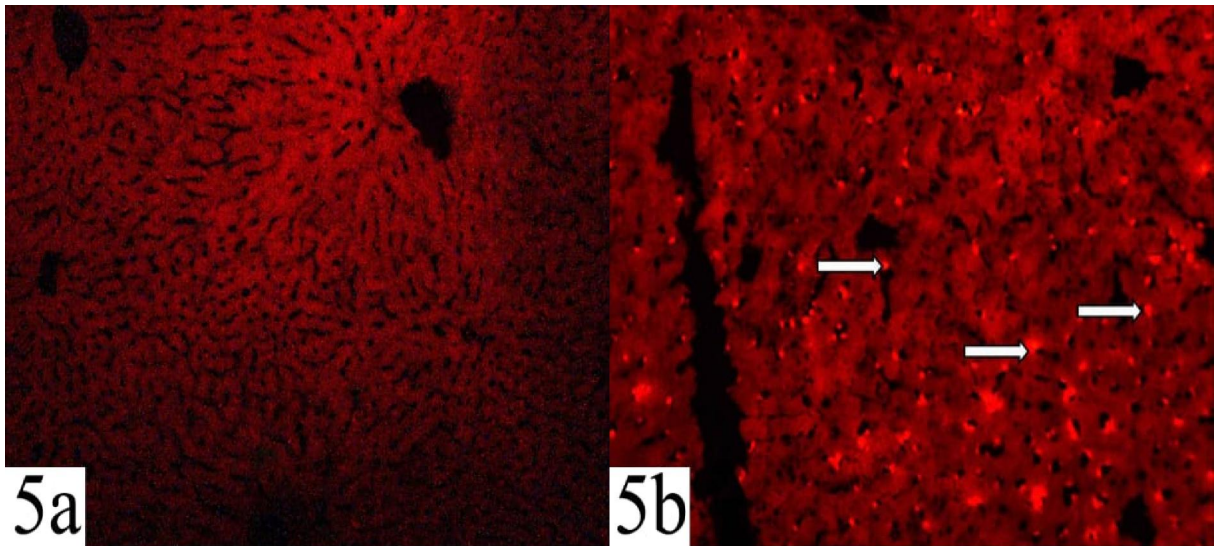


Figure 4: Photomicrographs of liver sections show positive immunoreaction in hepatocytes (thin arrows) and in inflammatory cells (arrow heads). [Group I (a & b), group II (c & d), subgroup IIIa (e & f), subgroup IIIb (g & h)]. [NF- κ B, x400 (a-h)]

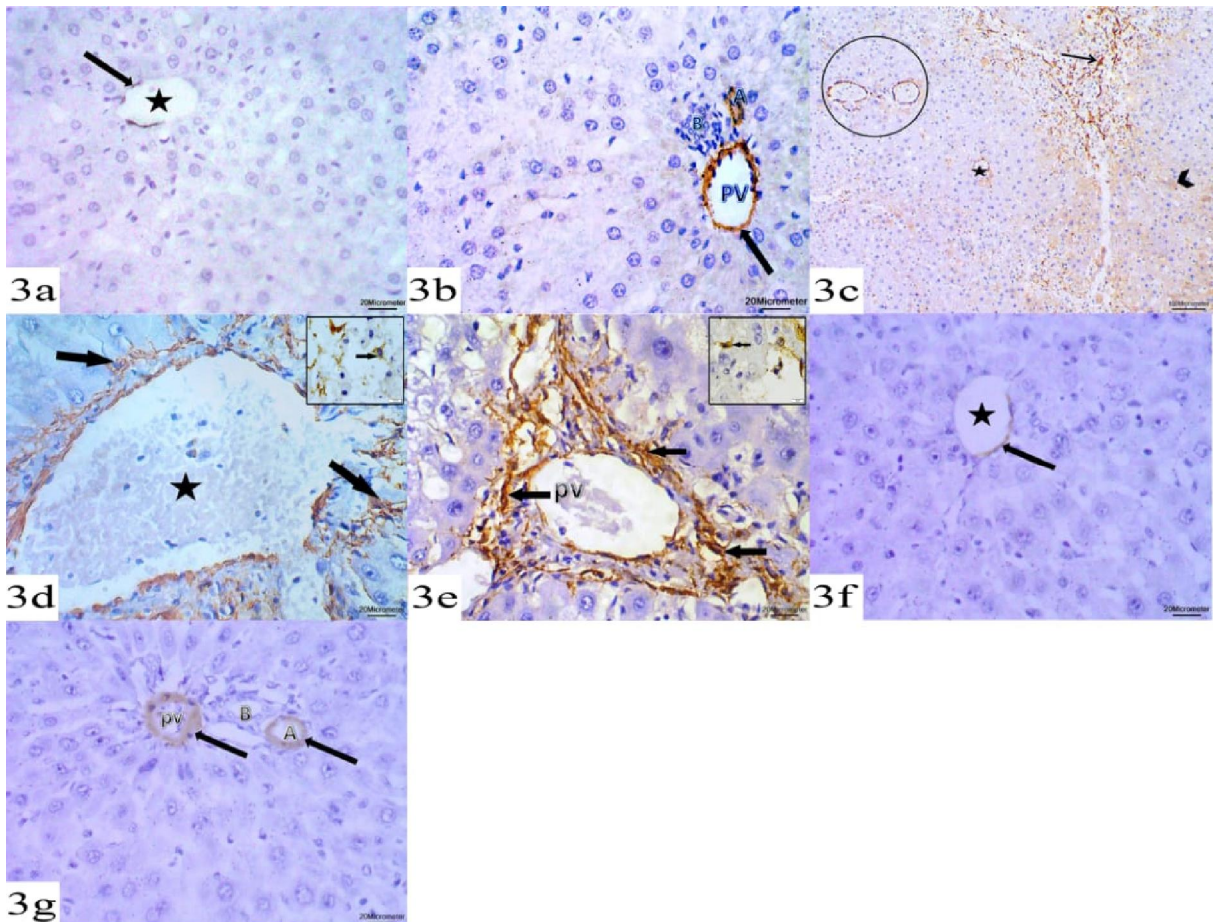


Figure 5: Photomicrographs of liver sections show PKH26 labelled AD-MSCs (thin arrows). [Subgroup Ie (a), subgroup IIIb (b)]. [Fluorescent staining, x200 (a & b)]

4. Discussion:

The liver is one of the most important organs in the human body as it is responsible for plasma protein synthesis, production of hormones, processing dead red blood cells, detoxification and glucose & lipid metabolism (**Abdou et al., 2015**).

Liver fibrosis is the response to hepatic injury, including alcohol abuse, viral infection and cholestasis. Experimentally it can be induced by administration of hepatotoxins such as TAA (**Al-Hashem et al., 2018**).

Mesenchymal stem cells, especially ADMSCs have become a prominent source in regenerative medicine and cell therapy. They provide an effective strategy for the treatment of an impaired liver (**Puglisi et al., 2011**).

Astragalus Membranaceus root extract has been used in Traditional Chinese medicine. It can resist collagen deposition and treat organ fibrosis by decreasing serum levels of transaminases and procollagen III in CCl₄ induced liver fibrosis (**Sun et al., 2007**).

In this study middle aged male albino rats were selected. This selection was done to exclude the effect of age and female sex hormones in liver regeneration. Estrogen was reported to effectively increase liver regeneration both *in-vivo* and *in-vitro*. It acts on its receptors present on hepatocytes regulating liver glucose and lipid homeostasis (**Shen and Shi, 2015**).

Group II of this study (received TAA for 8 weeks) showed marked hepatocytes injury. Such cellular injury coincides with the results of (**Czechowska et al., 2015 & Al-Attar and Shawush, 2015**) who used TAA to induce liver fibrosis.

It could be explained by oxidative stress that occur through different mechanisms. First, during TAA metabolism both flavin-containing monooxygenase and cytochrome P450 reduce dioxygen to superoxide anion and hydrogen peroxide causing oxidative hepatic damage (**Abdou et al., 2015**). Second, TAA is readily metabolized to reactive acetamide and thioacetamide-S-oxide. These metabolites combine covalently with macromolecules of the hepatic tissue leading to accumulation of fatty acids, damage of proteins and DNA and formation of reactive oxygen species leading to persistent oxidative stress (**Czechowska et al., 2015**). Third, TAA is converted into a highly toxic metabolite N-acetyl p-benzoquinone imine, through cytochrome p450 pathway. This metabolite is combined with glutathione (antioxidant) and excreted in the urine as conjugates causing rapid reduction of intracellular antioxidant glutathione.

The hepatocytes lesion occurred in this work was both apoptotic and necrotic. As hepatocytes were

either shrunken with pyknotic nuclei or swollen with dissolved nuclei). This finding is supported by **Moronvalle-Halley et al., (2005)** who proposed that administration of TAA to rodents could induce death by both apoptosis and necrosis simultaneously.

Apoptosis was proved to occur through either activation of death receptors such as Fas (**Liu and Pravia, 2010**) or imbalance between pro-apoptotic protein Bax and anti-apoptotic protein Bcl-2 expression mediating mitochondrial pathway of apoptosis (**David et al., (2011)**).

However, Necrosis appeared to be limited to a single row of hepatocytes surrounding the terminal hepatic venule (zone III) or extend up to half the width of the lobule (zone II) which was similarly reported by **Haschek et al., 2010**. They explained such central lobular necrosis by hypoxia/anoxia where oxygen tension is markedly decreased around the terminal hepatic venule, due to its consumption from the blood enters via the portal vein in the portal triad. Additionally, they added another explanation for such necrosis where uptake of toxins via the bile acid uptake pathway is located primarily in centrilobular hepatocytes.

Hepatocytes death detected in this study resulted in subsequent liver dysfunction. This functional deterioration was enforced by the significant decrease in albumin and significant increase in liver enzymes (AST & ALT) in this group versus control group. Such findings agree with those previously stated (**Abul et al., 2010 and Luo et al., 2015**) where the elevation of hepato-specific enzymes levels could be clarified by their release from the damaged hepatocytes to the blood. Moreover, the decreased serum albumin was suggested to be due to hepatocyte injury and dysfunction (**Al-Attar and Shawush, 2015**).

Hepatocytes oxidative stress stimulates Kupffer cells leading to production of proinflammatory cytokines, such as TNF- α and IL-6 (**Lee and Friedman, 2011**). Such cytokines result into inflammatory infiltration and activation of NF- κ B (**Orfila et al., (2005)**). The activated NF- κ B enhances the production of more proinflammatory cytokines and stimulates the expression of enzymes that increase the production of COX-2. Increased COX-2 leads to more cellular inflammation (**Shapiro et al., 2006; Luo et al., 2015; Algandaby, 2018**).

These data were enforced in this work by the detected prominent Kupffer cells, dilatation and congestion of the terminal hepatic venules, portal veins and hepatic sinusoids and the inflammatory cell infiltration seen in between the hepatic lobules. Additionally, there was strong positive NF- κ B immunoreactive hepatocytes and inflammatory cells

around both terminal hepatic venule and the branches of portal vein. This result was further supported by the significant increase in the mean area % of NF- κ B detected in this group versus control group.

Moreover, there were disorganization of lobular architecture and increase in the extracellular matrix collagen content in group II of the current study. These results were similarly reported previously (**Abdou et al., 2015**) and could be explained by the inflammatory cell infiltration proved to occur in between the hepatic lobules four weeks after TAA intake (**Mitsuhashi et al., 2004**). Further, HSCs were stated to be activated by the proinflammatory cytokines and OS and switched from an inactivate phenotype (vitamin A-storing cells) into proliferative (myofibroblast-like) cells (**Hyon et al., 2011; Algardaby, 2018**). The activated HSCs express α -SMA and considered as the major source of collagen and other matrix proteins that are deposited in fibrosis (**Dai et al., 2009**).

Such fibrotic changes were supported in this study by the significant increase in the mean area % of α -SMA positive activated HSCs in group II versus control group. Further enforcement came from the significant increase in the serum level of procollagen and mean area % of collagen fibers in Mallory trichrome stained sections in this group compared to control group.

Astragalus-treated subgroup (subgroup IIIa) of this work revealed marked improvement of the hepatic conditions with some abnormal changes. This finding is in accordance to that previously documented following CCL₄-induced hepatic fibrosis (**Sun et al., 2007**).

Such improvement could be enlightened by the significant antioxidant effect of AM detected in a former study (**Bratkov et al., 2016**). They proved that Astragaloside IV (one of the main components extracted from the Astragalus root) reduces the production of superoxide (O₂⁻), hydrogen peroxide (H₂O₂) with subsequent inhibition of membrane lipid peroxidation. This, in turn, decreased TNF- α production by Kupffer cells establishing the anti-inflammatory effect of AM (**Gui et al., 2006**) and its ability to inhibit NF- κ B activation (**Zhang and Frei, 2015; Liu et al., 2016 & Adesso et al., 2018**).

The anti-inflammatory action of AM was supported in the current work by the significant decrease in mean area % of NF- κ B versus group II.

These antioxidant and anti-inflammatory effects of AM could explain the nearly normal appearance of hepatocytes in this subgroup where they could prevent hepatocytes apoptosis as shown before (**Liu et al., 2014**). This was enforced in the current study by the significant increase in the serum level of albumin and significant decrease in AST & ALT levels in subgroup

IIIa than these in group II indicating liver functions improvement.

Reduction of TNF- α production by Kupffer cells with subsequent decrease in its pro-inflammatory cytokines release prevents the HSCs activation and transformation (**Lee et al., 2011**). Thus, AM could prevent collagen deposition and partially improve fibrosis as proved formerly in both *in vivo* and *in vitro* experiments on heart, liver, lungs, and kidneys (**Ren et al., 2013**). Additionally, Astragalus polysaccharides, another important constituent of Astragalus, could induce apoptosis in activated HSCs, and inhibit their proliferation (**Dang et al., 2009**).

Such anti-fibrotic effect of AM was supported in this work by the significant decrease in the plasma level of procollagen and mean area % of collagen and α -SMA in this subgroup when compared to untreated group II.

Stem cell-treated subgroup (subgroup IIIb) showed homing of PKH26 labeled stem cells in the liver. It also revealed nearly normal appearance of liver sections. These findings are in agreement with (**Muraca et al., 2007; Bergfeld et al., 2014**). They could be elucidated by the ability of AD-MSCs to inhibit the activation and proliferation of HSCs and promote their apoptosis. Such effect occurred not only via direct cell to cell contact but also through the trophic factors (IL-10, hepatocyte growth factor and nerve growth factor) secreted by AD-MSCs in its medium (**Yu et al., 2015**). These AD-MSCs effects would result into significant anti-fibrotic effect (**Jang et al., 2014; Yu et al., 2015**).

This anti-fibrotic effect of AD-MSCs was supported in the current study by the significant decrease in the serum level of procollagen and mean area % of collagen and α -SMA in this subgroup versus group II. These findings were similarly reported previously (**Jang et al., 2014; Yu et al., 2015**).

Moreover, MSCs were proved to undergo trans-differentiation into hepatic oval cells and then to hepatocyte-like cells. During this process, inflammation was reduced, damaged hepatocytes were repaired, and fibrosis was resolved, resulting in an overall improvement in liver function with a definite increase in intracellular glycogen storage (**El-Khayat et al., 2013 & Eom et al., 2015**). Furthermore, MSCs secreted cytokines and growth factors have an anti-apoptotic effect on hepatocytes and play an essential role in liver regeneration (**Mohammadi et al., 2012**).

This anti-inflammatory effect of AD-MSCs is due to the ability of the stem cells to suppress natural killer cell's proliferation (**Wang et al., 2012**) and B lymphocytes proliferation and differentiation into antibody-secreting cells (**Corcione et al., 2006**). Additionally, MSCs exert inhibitory effects on monocytes, dendritic cells, macrophages and NK cells,

which belong to the innate immune system (**Spaggiari et al., 2009**).

All these stem cells protective, anti-inflammatory and regenerative effects could improve the liver functions which was documented in this work by the significant increase in the serum level of albumin and significant decrease in serum levels of transaminases and mean area % of NF- κ B compared to group II.

In this work, all the biochemical and statistical results of subgroup IIIb (stem cell-treated subgroup) showed significant improvement than that of subgroup IIIa (Astragalus-treated subgroup). This might be explained by that Astragalus is a herb taken orally. So, it needs more time to achieve an effect like stem cells. In addition to the more potent anti-inflammatory and anti-fibrotic effects of stem cells that reported in previous studies (**Abdel Aziz et al., 2007; Jang et al., 2014**).

References:

1. Abdou ES, Taha MN, Mandour AWEA, Lebda AM, El Hofi RH and El-Morshedy MSEA (2015): Antifibrotic Effect of Curcumin on Thioacetamide Induced Liver Fibrosis Alexandria. *Journal Of Veterinary Sciences*, 45(1):43-50.
2. Al-Attar AM and Shawush NA (2015): Influence of olive and rosemary leaves extracts on chemically induced liver cirrhosis in male rats. *Saudi J BiolSci*, 22(2): 157–163.
3. Alshawsh MA, Abdulla MA, Ismail S and Amin ZA (2011): Hepatoprotective effects of orthosiphonstamineus extract on thioacetamide-induced liver cirrhosis in rats. *Evid Based Complement Alternat Med*. 2011:103039. doi: 10.1155/2011/103039.
4. Algendaby MM (2018): Antifibrotic effects of crocin on thioacetamide-induced liver fibrosis in mice. *Saudi Journal of Biological Sciences*, 25(4):747-757.
5. Armitage P, Berry G and Matthews JNS (2001): *Statistical methods in medical research*. 4thed, Wiley Blackwell: 1-832.
6. Al-Hashem F, Alhumayed S, Ellatiff MA, Amin SN, Kamar SS, Al-Ani B and Haidara MA (2018): Metformin protects against thioacetamide-induced liver injury in rats. *Int. J. Morphol*, 36(3):984-990.
7. Abul K, Najmi KK and Pillai SN (2010): Effect of lornithine aspartate against thioacetamide-induced hepatic damage in rats. *Indian J Pharm*, 42(6): 384-387.
8. Adesso S, Russo R, Quaroni A, Autore G and Marzocco S (2018): Astragalusmembranaceus Extract Attenuates Inflammation and Oxidative Stress in Intestinal Epithelial Cells via NF- κ B Activation and Nrf2 Response. *Int J MolSci*, 19(3): 800.
9. Abdel Aziz MT, Atta HM, Mahfouz S, Fouad HH, Roshdy NK, Ahmed HH, Rashed LA, Sabry D, Hassouna AA and Hasan NM (2007): Therapeutic potential of bone marrow-derived mesenchymal stem cells on experimental liver fibrosis. *ClinBiochem*, 40(12): 893–899.
10. Corcione A, Benvenuto F, Ferretti E, Giunti D, Cappiello V, Cazzanti F, Risso M, Gualandi F, Mancardi GL, Pistoia V and Uccelli A (2006): Human mesenchymal stem cells modulate B-cell functions. *Blood*, 107(1): 367-372.
11. El-khayat Z, Mostafa E, Hussein J, El-Wassef M, Rashed L, Farrag RA and Medhat D (2013): Mesenchymal Stem cells Therapy for Thioacetamide Induced Liver Cirrhosis. *Korean J Intern Med*, 5(2): 975-1491.
12. Eom WY, Shim YK and Baik KS (2015): Mesenchymal stem cell therapy for liver fibrosis. *Korean J Intern Med*, 30(5): 580–589.
13. Bergfeld AS, Blavier L and De-Clerck AY (2014): Bone Marrow-Derived Mesenchymal Stromal Cells Promote Survival and Drug Resistance in Tumor Cells *Cancer Biology and Signal Transduction*. *Mol Cancer Ther*, 13(4): 962–975.
14. Dang SS, Jia XL, Song P, Cheng YA Zhang X Sun MZ and Liu EQ (2009): Inhibitory effect of emodin and Astragalus polysaccharide on the replication of HBV. *World J Gastroenterol*, 15(45): 5669-5673.
15. Bratkov VM, Shkondrov AM, Zdraveva PK and Krasteva IN (2016): Flavonoids from the Genus Astragalus: Phytochemistry and Biological Activity, 10(19):11-32.
16. Dai LJ, Li HY, Guan LX, Ritchie G and Zhou JX (2009): The therapeutic potential of bone marrow-derived mesenchymal stem cells on hepatic cirrhosis. *Stem Cell Res*, 2(1): 16–25.
17. David C, Rodrigues G and Bona S (2011): Role of Quercetin in Preventing Thioacetamide-Induced Liver Injury in Rats. *Toxicologic Pathology*, 39(6): 949-957.
18. Czechowska G, Celinski K, Korolczuk A, Wojcika G, Dudka J, Bojarska A and Reiter RG (2015): Protective effects of melatonin against thioacetamide-induced liver fibrosis in rats. *Journal of physiology and pharmacology*, 66(4): 567-579.
19. Cherg S, Young J and Ma H (2008): Alpha-Smooth Muscle Actin (α -SMA). *The Journal of American Science*, 4(4):1545-1003.
20. Bancroft J and Gamble M (2008): *Theory and practice of histological techniques*. 6thed.

- Churchill-Livingstone, London, England: 147-150.
21. Bunnell BA, Flaata M, Gagliardi C, Patel C and Ripoll C (2008): Adipose- derived stem cells: isolation expansion and differentiation. *Methods*, 45(2):115-120.
 22. Cheng Y, Mai JY, Wang MF, Chen GF and Ping J. (2017): Antifibrotic effect of total flavonoids of *Astragalus Radix* on dimethylnitrosamine-induced liver cirrhosis in rats. *Chin J Integrative Med*, 23:48.
 23. Bataller R and Brenner AD (2005): Liver fibrosis. *J Clin Invest*, 115(2):209–218.
 24. Blaner WS, O'Byrne SM, Wongsiriroj N, Kluwe J, D'Ambrosio DM, Jiang H, Schwabe RF, Hillman EM, Piantedosi R and Libien J(2009): Hepatic stellate cell lipid droplets: a specialized lipid droplet for retinoid storage. *Biochim Biophys Acta*, 1791(6):467–473.
 25. Gines P, Cardenas A, Arroyo V and Rodes J (2004): Management of cirrhosis and ascites. *N Engl J Med*, 350:1646–1654.
 26. Kiernan JA (2015): *Histological and histochemical methods: Theory and practice*. 5th ed. Scion Publishing Ltd, Banbury, UK: 571.
 27. Haschek MW, Rousseaux CG and Wallig AM (2010): Chapter 9. Liver. In *Fundamentals of Toxicologic Pathology* 2nded:197-235.
 28. Hyon MK, Kwon E, Choi HJ and Kang BC (2011): Dimethylnitrosamine-Induced Liver Fibrosis and Recovery in NOD/SCID Mice. *J Vet MedSci*, 73(6):739-745.
 29. Gui SY, Wei W, Wang H, Wu L, Sun WY, Chen WB and Wu CY (2006): Effects and mechanisms of crude *Astragalosides* fraction on liver fibrosis in rats. *J Ethnopharmacol*, 103(2):154–159.
 30. Jang OY, Kim YM, Cho YM, Baik KS, Cho ZY and Kwon OS (2014): Effect of bone marrow-derived mesenchymal stem cells on hepatic fibrosis in a thioacetamide-induced cirrhotic rat model. *BMC Gastroenterology*, 14:198. doi: 10.1186/s12876-014-0198-6.
 31. Spaggiari GM, Abdelrazik H, Becchetti F and Moretta L (2009): MSCs inhibit monocyte-derived DC maturation and function by selectively interfering with the generation of immature DCs: central role of MSC-derived prostaglandin E2. *Blood*, 113 (26): 6576-6583.
 32. Ross MH and Pawlina W (2016): Chapter 18. Digestive System III: Liver, Gallbladder and Pancreas. In: *Histology: a text and atlas, with correlated cell and molecular biology*. 7thed. Lippincott William & Wilkins, Wolters Kluwer business. Philadelphia, USA: 626-661.
 33. Ren S, Zhang H, Mu Y, Sun M and Liu P (2013): Pharmacological effects of *Astragaloside IV*: a literature review. *J Tradit Chin Med*, 33(3): 413-416.
 34. Sun WY, Wei W, Wu L, Gui SY and Wang H (2007): Effects and mechanisms of extract from *Paeonialactiflora* and *Astragalus membranaceus* on liver fibrosis induced by carbon tetrachloride in rats. *J Ethnopharmacol*, 112(3):514–523.
 35. Shapiro H, Ashkenazi M, Weizman N, Shahmurov M, Aeed H and Bruck R (2006): Curcumin ameliorates acute thioacetamide-induced hepatotoxicity. *Journal of Gastroenterology and Hepatology*, 21(2):358–366.
 36. Orfila C, Lepert JC, Alric L, Carrera G, Béraud M and Pipy B (2005): Immunohistochemical distribution of activated nuclear factor kappa B and peroxisome proliferator-activated receptors in carbon tetrachloride-induced chronic liver injury in rats. *Histochem Cell Biol*, 123(6): 585–593.
 37. Puglisi MA, Tesori V, Lattanzi W, Piscaglia AC, Gasbarrini GB, D'Ugo DM and Gasbarrini A (2011): Therapeutic implications of mesenchymal stem cells in liver injury. *J Biomed Biotechnol*, 2011:860578. doi: 10.1155/2011/860578.
 38. Shen M and Shi H (2015): Sex Hormones and Their Receptors Regulate Liver Energy Homeostasis. *Int J Endocrinol*:2015:294278. doi: 10.1155/2015/294278.
 39. Ramos-Vara JA and Miller MA (2014) "When tissue antigens and antibodies get along: revisiting the technical aspects of immunohistochemistry--the red brown and blue technique". *Veterinary Pathology*, 51 (1): 42–87.
 40. Tseng A, Yang C, Chen C, Hsu L, Lee M, Lee H and Su L, (2016): An *in vivo* molecular response analysis of colorectal cancer treated with *Astragalus Membranaceus* extract. *Oncol Rep*, 35(2): 659–668.
 41. Lee UE and Friedman SL (2011): Mechanisms of hepatic fibrogenesis. *Best Pract Res Clin Gastroenterol*, 25(2):195-206.
 42. Liedtke C, Luedde T, Sauerbruch T, Scholten D, Streetz D, Tacke F, Tolba R, Trautwein C, Trebicka J and Weiskirchen R (2013): Experimental liver fibrosis research: update on animal models legal issues and translational aspects. *Fibrogenesis & Tissue Repair*, 6 (1):1-19.
 43. Miryounesi M, Piryaei A, Pournasr B, Aghdami N and Baharv H (2013): Repeated versus single transplantation of mesenchymal stem cells in carbon tetrachloride – induced liver injury in mice. *Cell Biol Int*, 37(4): 340-347.

44. Meng LQ, Tang JW, Wang Y, Zhao JR, Shang MY, Zhang M, Liu SY, Qu L, Cai SQ and Li XM (2011): Astragaloside IV synergizes with ferulic acid to inhibit renal tubule interstitial fibrosis in rats with obstructive nephropathy. *Br J Pharmacol*, 162(8): 1805-1818.
45. Moronvalle-Halley V, Sacre-Salem B, Sllez V, Labbe G and Gautier J (2005): Evaluation of cultured precision-cut rat liver slices as a model to study drug induced liver apoptosis. *Toxicol*, 207(2):203-214.
46. Liu RM and Pravia KA (2010): Oxidative stress and glutathione in TGF-b-mediated fibrogenesis. *Free Radical Biol Med*, 48 (1):1-15.
47. Luo M, Dong L, Li J, Wang Y and Shang B (2015): Protective effects of pentoxifylline on acute liver injury induced by thioacetamide in rats. *Int J ClinExp Path*, 8(8): 8990–8996.
48. Mitsuhashi M, Morimura K, Wanibuchi H, Kiyota A, Wada S, Nakatani T and Fukushima S (2004): Examination of the Rat Model of Liver Injury via Thioacetamide TAA or Carbon Tetrachloride CCl₄. *J Toxicol Pathol*, 17:219-222.
49. 142) Liu HC, Shi HE, Huang F, Peterson EK, Wu H, Lan YY, Zhang BB, He YX, Woods T, Du M, Wu XJ and Wang ZT (2016): Astragaloside IV inhibits microglia activation via glucocorticoid receptor mediated signaling pathway. *Sci Rep*, 6: 19137. doi: 10.1038/srep19137.
50. Liu W, Gao FF, Li Q, LV WJ, Wang Y, Hu CP, Xiang MQ and Wei L (2014): Protective Effect of Astragalus Polysaccharides on Liver Injury Induced with Different Chemotherapeutics in Mice. *Asian Pac J Cancer Prev*, 15 (23): 10413-10420.
51. Lee JH, Lee H, Joung YK, Jung KH, Choi JH, Lee DH, Park KD and Hong SS (2011): The use of low molecular weight heparin-pluronicnanogels to impede liver fibrosis by inhibition the TGF-beta/Smad signaling pathway. *Biomaterials*, 32(5):1438–1445.
52. Soresi M, Giannitrapani L, Cervello M, Licata A and Montalto G (2014): Non invasive tools for the diagnosis of liver cirrhosis, *World J Gastroenterol*, 20(48): 18131–18150.
53. Muraca M, Ferrareso C, Vilei MT, Granato A, Quarta M, Cozzi E, Rugge M, Pauwelyn KA, Caruso M, Avital I, Inderbitzin D, Demetriou AA, Forbes SJ and Realdi G (2007): Liver repopulation with bone marrow derived cells improves the metabolic disorder in the Gunn rat. *Gut*, 56(12):1725-1735.
54. Mohammadi GS, Karimpor MAA, Hashemi-Soteh MB, Rafiei A, Parivar K and Aghdami N (2012): Effect of mesenchymal stem cells on doxorubicin-induced fibrosis. *Cell J*, 14(2):142–151.
55. Wang PP, Xie DY, Liang XJ, Peng L, Zhang GL, Ye YN, Xie C and Gao ZL (2012): HGF and direct mesenchymal stem cells contact synergize to inhibit hepatic stellate cells activation through TLR4/NF-kB pathway. *PLoS One*, 7(8): 43408.
56. Yu F, Ji S, Su L, Wan L, Zhang S, Dai C, Wang Y, Fu J and Zhang Q (2015): Adipose-derived mesenchymal stem cells inhibit activation of hepatic stellate cells *in vitro* and ameliorate rat liver fibrosis *in vivo*. *Journal of the Formosan Medical Association*, 114(2): 130-138.
57. Yang BH, Zhu LQ, Zhang JZ, Niu FL and Cui W (2005): Effects of Astragalus Membranaceus and Panaxnotoginseng on the transformation of bone marrow stem cells and proliferation of EPC *in vitro*. *Zhongguo Zhong Yao Za Zhi*, 30 (22):1761-1763.
58. Ionescu AG, Streba MAL, Vere CC, Ciurea ME, Streba CT, Ionescu M, Comanescu M, Irimia E and Rogoveanu E (2013): Histopathological and immunohistochemical study of hepatic stellate cells in patients with viral C chronic liver disease. *Rom J Morphol Embryol*, 54(4):983–991.
59. Zuk PA, Zhu M, Ashjian P, De Ugarte DA, Huang JI, Mizuno H, Alfonso ZC, Fraser JK, Benhaim P and Hedrick MH (2002): Human adipose tissue is a source of multipotent stem cells. *Mol Biol Cell*, 13: 4279–4295.
60. Zhang WJ and Frei B (2015): Astragaloside IV Inhibits NF- κ B Activation and Inflammatory Gene Expression in LPS-Treated Mice. *Mediators of Inflammation*, 2015: 274314. doi: 10.1155/2015/274314.